# Radiogenic Neutron Background v2.1

J. Cooley,[3] D.-M. Mei,[4] K.J. Palladino,[2] H. Qiu,[3] M. Selvi,[1] S. Scorza,[3,5] C. Zhang,[4] and ....
(The AARM Collaboration)
[1]*INFN - Sezione di Bologna, Italy*
[2]*Department of Physics, University of Wisconsin-Madison, Madison, WI 53706, USA*
[3]*Department of Physics, Southern Methodist University, Dallas, TX 75275, USA*
[4]*Department of Physics, University of South Dakota, Vermillion, USA*
[5]*Karlsruhe Institute of Technology, Institute of Experimental Nuclear Physics, Gaedestr. 1, 76128 Karlsruhe, Germany*
(Dated: February 25, 2016)

Ultra-low-background experiments, generically termed rare-event searches, address some of the most important open questions in particle physics, cosmology and astrophysics: direct detection of dark matter, neutrinoless double beta decay, proton decay, and detection of solar and supernovae neutrinos. Although their detection methods and physics goals are varied, rare-event searches share a number of common requirements in order to obtain sensitivity to low-rate processes in the presence of an overwhelming rate of environmental radiation, including the need for significant rock overburdens to moderate the flux of cosmic-ray muons. This requirement is so universal that an international community of underground science has emerged, with dozens of experiments operating in mines that vary in depth from a few hundred to many thousand meters water equivalent (m.w.e.) .

Simulations are used to understand backgrounds caused by naturally occurring radioactivity in the rock and in every piece of shielding and detector material used in the experiment. Most important are processes like spontaneous fission and ($\alpha$,n) reactions in material close to the detectors that can produce neutrons. A comparison study between two dedicated softwares is detailed. Neutron yields and spectra obtained with Mei-Zhang-Hime and SOURCES4 codes are presented.

## I. INTRODUCTION

Reduction of radiogenic backgrounds is one of the most important factors for rare event search experiments including searches for dark matter and neutrino-less double beta decay. These radiogenic backgrounds can be generically classified into two types: electron recoil and nuclear recoil backgrounds. Electron recoil backgrounds result from the interactions of gamma rays, electrons or beta particles interacting with the electrons in the detector's target medium while nuclear recoil backgrounds result from neutrons interacting with the nucleus in the detector's target medium. In dark matter experiments, the nuclear recoil background is of particular concern because a nuclear recoil from a neutron can be indistinguishable from a nuclear recoil from a WIMP.

Neutrons are produced by spontaneous fission, $\alpha$-n interactions and muon-induced interactions. Muon-induced neutrons can be reduced by operation the detector deep underground and by placing passive shielding around the detector. In addition, muon-induced neutrons can often be recognized by identifying the parent muon in a muon veto. More difficult to deal with are neutrons resulting from $\alpha$-n interactions and spontaneous fission from $^{238}$U, $^{235}$U, and $^{232}$Th present in the materials used to construct the shielding and the detectors themselves. Thus, experimentalists must select their materials carefully when designing and constructing their experiments. This requires that they have accurate simulations of the processes in the materials they are considering.

There are currently two codes available for use in such calculations, SOURCES-4 [1] and a second code developed by Mei, Zhang and Hei [2] which we will refer to as the USD code.

## II. NEUTRON YIELD AND SPECTRA

The measurements of neutron spectra strongly depend on the material and are not straightforward since neutrons are neutral particles. Their calculations are critical for low background experiments. The total neutron yield indicates the number of neutrons which are produced or had entered the target whereas the neutron energy spectrum determines the background events we would expect in the energy range of interest. Both are needed in order to carry out a complete and reliable neutron background simulation. The evaluation of neutron yields and spectra can be performed via different codes: the modified version of SOURCES4A and the code developed by Mei, Zhang and Hime made available online at http://neutronyield.usd.edu have been considered. SOURCES4 code has been modified to extend the cross section for ($\alpha$,n) up to 10 MeV, based on experimental data, whenever possible, and calculations performed via the EMPIRE code [3] by the group at the University of Sheffield. The SOURCES4A and USD codes calculate neutron yields and spectra from ($\alpha$, n) reactions due to the decay of radionuclides. Radiogenic neutrons result from the decay of the intrinsic contamination of materials surrounding the detectors with $^{232}$Th, $^{238}$U and $^{235}$U. A comparison study between SOURCES4 and USD codes is carried out considering the $^{232}$Th and the $^{238}$U decay chains in secular equilibrium, although a possibility of disequilibrium can be taken into account: due to different migration, the long-lived isotopes, $^{226}$Ra, $^{222}$Rn, $^{210}$Po, $^{228}$Ra, $^{228}$Th and their associated decay daughters could be calculated separately, see table I. For both chains, most of the neutrons are produced by the $\alpha$ generated in the second part of the chains.

TABLE I. Radiogenic neutron yield (n·s$^{-1}$·cm$^{-3}$) from ($\alpha$, n) reactions in different materials for 1ppb of $^{238}$U and $^{232}$Th decay chains. Neutron yields have been calculated via the modified SOURCES4A code.

| **Material** | **Neutron yield for 1ppb (n·s$^{-1}$·cm$^{-3}$)** $^{238}$U → $^{226}$Ra | $^{226}$Ra → $^{206}$Pb |
|---|---|---|
| Stainless Steel | $6.4 \cdot 10^{-15}$ | $3.1 \cdot 10^{-11}$ |
| Pyrex | $4.0 \cdot 10^{-11}$ | $1.9 \cdot 10^{-10}$ |
| Borosilicate Glass | $6.3 \cdot 10^{-11}$ | $2.8 \cdot 10^{-10}$ |
| Titanium | $1.14 \cdot 10^{-13}$ | $1.0 \cdot 10^{-10}$ |
| Copper | $0.0 \cdot 10^{-11}$ | $2.8 \cdot 10^{-12}$ |
| PE ($C_2H_4$) | $1.6 \cdot 10^{-12}$ | $1.1 \cdot 10^{-11}$ |
| PTFE ($CF_2$) | $1.8 \cdot 10^{-10}$ | $1.6 \cdot 10^{-9}$ |
| | **$^{232}$Th → $^{228}$Th** | **$^{228}$Th → $^{208}$Pb** |
| Stainless Steel | $8.8 \cdot 10^{-19}$ | $4.1 \cdot 10^{-11}$ |
| Pyrex | $2.4 \cdot 10^{-12}$ | $8.4 \cdot 10^{-11}$ |
| Borosilicate Glass | $3.8 \cdot 10^{-12}$ | $1.2 \cdot 10^{-10}$ |
| Titanium | $4.4 \cdot 10^{-16}$ | $9.3 \cdot 10^{-11}$ |
| Copper | $0.0 \cdot 10^{-11}$ | $9.5 \cdot 10^{-12}$ |
| PE ($C_2H_4$) | $1.6 \cdot 10^{-13}$ | $5.1 \cdot 10^{-12}$ |
| PTFE ($CF_2$) | $7.1 \cdot 10^{-12}$ | $7.7 \cdot 10^{-10}$ |

The calculation of the neutron spectra requires as inputs the cross-sections of ($\alpha$, n) reactions, the probabilities of nuclear transition to different excited states (branching ratios) and the alpha emission lines from the radioactive radionuclides. Both codes consider a thick target: calculation of neutron yields and spectra are carried out under the assumption that the size of radioactive sample exceeds significantly the range of the alpha particle. The energy bin size of the ($\alpha$, n) calculation is fixed to be 0.1 MeV in USD code while is user dependent in SOURCES4A.

Table II lists the $\alpha$-lines respectively resulting from the $^{232}$Th and $^{238}$U decay chains that are present in SOURCES4A and USD codes. USD code is missing the $\alpha$-lines from the $^{222}$Ra isotope in the $^{238}$U decay chain that is considered by the SOURCES4A library. Overall, the branching ratio and the energy lines are in good agreement between the two codes.

Cross-sections and branching ratios are required for neutron yield and spectra calculations as well. The USD code uses TENDL 2012 [4] to provide ($\alpha$, n) nuclear cross-sections. TENDL is a validated nuclear data library which provides the output of the TALYS [5] nuclear model code system; the SOURCES4 cross section input libraries come from EMPIRE2.19 [3] calculations and, for some isotopes, a combination of data measurements and EMPIRE2.19 calculations. Also, EMPIRE is the code recommended by International Atomic Energy Agency (IAEA). Neither EMPIRE nor TALYS can

TABLE II. Alpha lines present in SOURCES4A and USD, and their intensity (BR) for isotopes in the $^{232}$Th and $^{238}$U decay chains. Only lines with intensity $> 1\%$ have been quoted.

| **Isotopes** | **SOURCES4A Line (keV)** | **BR (%)** | **USD Line (MeV)** | **BR (%)** |
|---|---|---|---|---|
| **$^{238}$U** | 4151 | 21 | 4.151 | 21 |
| | 4198 | 79 | 4.198 | 79 |
| **$^{234}$U** | 4722.4 | 28.42 | 4.722 | 28.6 |
| | 4774.6 | 71.38 | 4.775 | 71.4 |
| **$^{230}$Th** | 4620.5 | 23.4 | 4.621 | 23.7 |
| | 4687.0 | 76.3 | 4.688 | 76.3 |
| **$^{226}$Ra** | 4601 | 5.55 | 4.602 | 5.6 |
| | 4784.34 | 94.45 | 4.784 | 94.4 |
| **$^{222}$Rn** | 5489 | 99.92 | 5.490 | 100 |
| **$^{218}$Po** | 6002.35 | 99.98 | 6.002 | 100 |
| **$^{214}$Po** | 7686.82 | 99.99 | 7.687 | 99.99 |
| **$^{210}$Po** | 5304.33 | 99.99 | 5.304 | 100 |
| **$^{232}$Th** | 3947.2 | 21.7 | 3.954 | 22.1 |
| | 4012.3 | 78.2 | 4.013 | 77.9 |
| **$^{228}$Th** | 5340.36 | 27.2 | 5.340 | 28.5 |
| | 5423.15 | 72.2 | 5.423 | 71.5 |
| **$^{224}$Ra** | 5448.6 | 5.06 | 5.449 | 5.1 |
| | 5685.37 | 94.92 | 5.685 | 94.9 |
| **$^{220}$Rn** | 6288.3 | 99.99 | 6.288 | 100 |
| **$^{216}$Po** | 6778.5 | 99.99 | 6.778 | 100 |
| **$^{212}$Bi** | 6051.1 | 25.16 | 6.050 | 26.2 |
| | 6090.2 | 9.79 | 6.0902 | 9.8 |
| **$^{212}$Po** | 8784.6 | 100 | 8.784 | 64 |

TABLE III. Radiogenic neutron yield (n/s/cm$^3$) for copper and polyethylene materials and for $^{238}$U and $^{232}$Th decay chains. Column (1) and (2) refer to pure USD and SOURCES4A calculation, respectively. Column (3) refers to SOURCES4A calculation with USD ($\alpha$, n) cross section libraries. A ratio of the neutron yield is also provided: column (a) refers to the ratio of (2) over (1), whereas column (b) corresponds to the ratio (2)/(3)

| **Material** | **Chain** | **Neutron Yield ($10^{-12}$· n·s$^{-1}$·cm$^{-3}$)** (1) | (2) | (3) | **Ratio** (a) | (b) |
|---|---|---|---|---|---|---|
| Copper | $^{238}$U | 3.46 | 2.84 | 2.93 | 0.8 | 1.0 |
| | $^{232}$Th | 11.1 | 9.49 | 9.18 | 0.9 | 1.0 |
| Polyethylene ($C_2H_4$) | $^{238}$U | 9.56 | 12.6 | 16.4 | 1.3 | 0.8 |
| | $^{232}$Th | 2.87 | 5.28 | 5.97 | 1.8 | 0.9 |

properly calculate all resonance behavior which has been experimentally observed.

An extensive comparison between the different cross-section libraries used in USD and SOURCES4A has been carried out for the target nuclides present in the materials contributing the most to radiogenic neutron backgrounds. Specifically, we refer to materials which compose the shielding scheme and the internal detector parts, such as stainless steel, copper, titanium, borosilicate glass (PMTs glass), and PTFE, which become important when the external flux is attenuated by the shielding. Comparison of cross section inputs results in a good agreement

FIG. 1. Input ($\alpha$, n) cross-section for the target isotopes involved in radiogenic neutron calculations for copper and polyethylene. Red markers refers to SOURCES4A inputs, whereas the black markers to USD. From left to right, top to bottom: $^{63}$Cu, $^{65}$Cu, $^{13}$C, $^{19}$F, $^{10}$B and $^{11}$B.

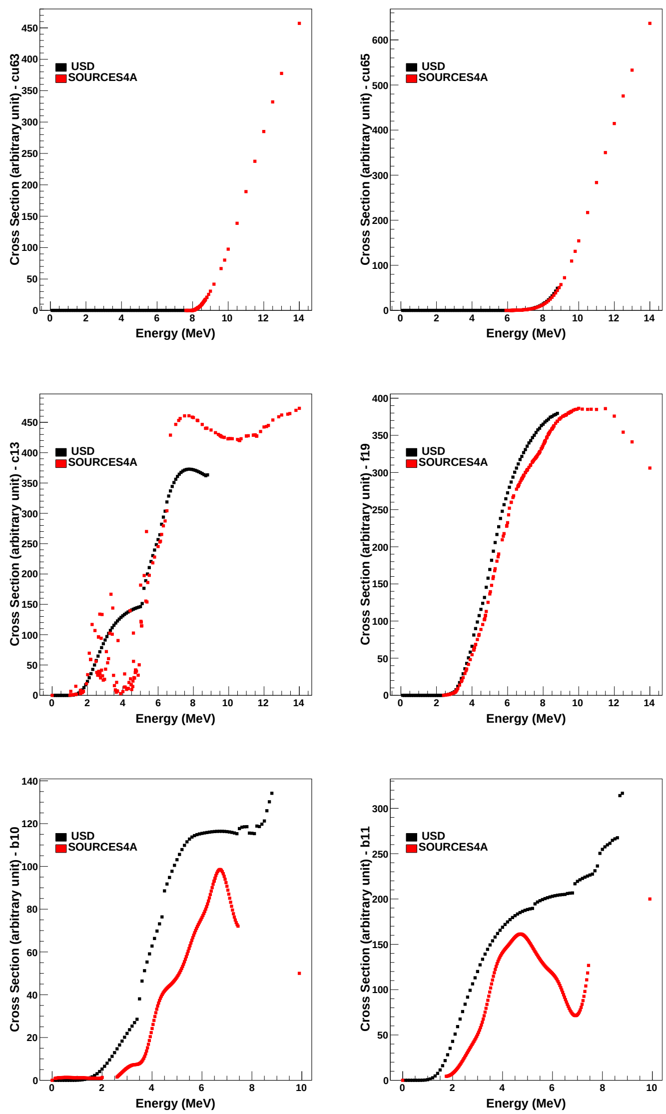


for most of isotopes in both code libraries. For some, such as $^{13}$C and $^{10}$B and $^{11}$B the cross sections show discrepancies. To better understand the contribution due to the cross section input library in the radiogenic neutron yield and spectrum we have calculated radiogenic neutron yield and spectra for two different materials: copper, for which the input cross sections in both codes are matching, and polyethylene, for which input cross sections of $^{13}$C show discrepancies between the codes, details in figure 1. We have considered natural copper (70% $^{63}$Cu and 30% $^{65}$Cu) with a density of 8.96 g/cm$^3$; polyethylene material ($C_2H_4$) is considered with a density

FIG. 2. Radiogenic neutron spectra (n$\cdot$MeV$^{-1}\cdot$s$^{-1}\cdot$cm$^{-3}$) calculated for 1ppb $^{238}$U and $^{232}$Th decay chains, left and right panels, respectively. First row show copper contribution, lower row polyethylene material. Dotted blu lines refers to pure USD calculations, plain orange line to pure SOURCES4A calculations and dashed green line is the mixed computation for which we ran SOURCES4A algorithm with input cross section of USD code.

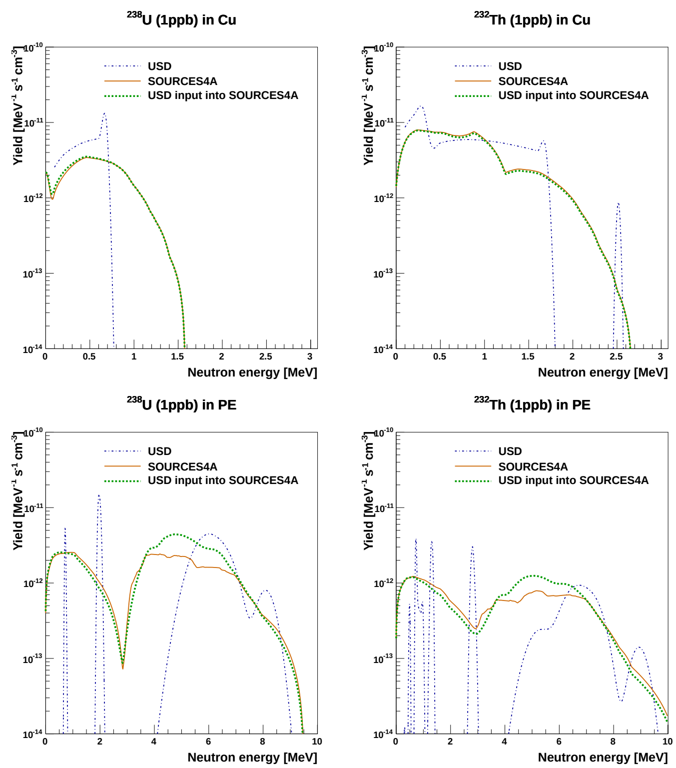


of density is 0.935 g/cm$^3$. Estimates are done for 1ppb in $^{238}$U and $^{232}$Th decay chains. Calculations consist of pure SOURCES4A and USD computation and a mixed computation for which we run SOURCES4A algorithm with cross section inputs of USD. Resulting radiogenic neutron yields are quoted in table III. The column (a) of the radiogenic neutron yield ratio quotes the calculation differences between SOURCES4A and USD codes: they show a reasonably good agreement, within a 50% discrepancy. The column (b) refers to the ratio of radiogenic neutron yield resulting from the same algorithm calculation (SOURCES4A) but with USD (column (3)) and SOURCES4A (column (2)) input ($\alpha$, n) cross-sections. For polyethylene, we can conclude that the input cross-section may account up to a 20% discrepancy in neutron yield. Figure 3 shows radiogenic neutron spectra for copper (upper row) and polyethylene (lower row), both from uranium and thorium decay chains, left and right panels respectively.

A comparison of neutron yield and energy spectra obtained via SOURCES4A and USD codes for different materials has been carried out. Results are shown in table IV and figure 3. A qualitative agreement between the two codes is observed. A maximum discrepancy of a factor 2 is found. The energy spectra calculated via SOURCES4A code are in general smoother, without the presence of resonant peaks, a prominent feature of the USD spectra.

TABLE IV. Radiogenic neutron yield ($n{\cdot}s^{-1}{\cdot}cm^{-3}$) per material considering 1ppb of $^{238}U$ and $^{232}Th$. The percentage difference is calculates as (SOURCES4A-USD)/[(SOURCES4A+USD)/2].

| **Material** | **Chain** | **Neutron Yield ($n{\cdot}s^{-1}{\cdot}cm^{-3}$)** SOURCES4A | USD | Diff % |
|---|---|---|---|---|
| Cu | $^{238}U$ | 2.84E-12 | 3.46E-12 | 20 |
| | $^{232}Th$ | 9.49E-12 | 1.11E-11 | 16 |
| PE ($CH_2$) | $^{238}U$ | 1.26E-11 | 9.56E-12 | -27 |
| | $^{232}Th$ | 5.28E-12 | 2.87E-12 | -59 |
| Titanium | $^{238}U$ | $1.04\ 10^{-10}$ | $1.99\ 10^{-10}$ | -63 |
| | $^{232}Th$ | $9.29\ 10^{-11}$ | $1.24\ 10^{-10}$ | -28 |
| Stainless Steel | $^{238}U$ | $3.10\ 10^{-11}$ | $5.95\ 10^{-11}$ | -63 |
| | $^{232}Th$ | $4.05\ 10^{-11}$ | $6.80\ 10^{-11}$ | -51 |
| Pyrex | $^{238}U$ | $2.30\ 10^{-10}$ | $1.61\ 10^{-10}$ | 36 |
| | $^{232}Th$ | $8.66\ 10^{-11}$ | $4.59\ 10^{-11}$ | 61 |
| Borosilicate Glass | $^{238}U$ | $3.48\ 10^{-10}$ | $2.45\ 10^{-10}$ | 35 |
| | $^{232}Th$ | $1.27\ 10^{-10}$ | $6.98\ 10^{-11}$ | 58 |
| PTFE ($CF_2$) | $^{238}U$ | $1.81\ 10^{-9}$ | $1.60\ 10^{-9}$ | 12 |
| | $^{232}Th$ | $7.76\ 10^{-10}$ | $5.42\ 10^{-10}$ | 36 |

## III. GEANT4 PROPAGATION

To evaluate the impact of the varying neuron spectra produced by SOURCES4A and the USD calculator, simplified detector geometries were created within a RAT [6] framework with Geant4.9.5.p01 and the pertinent high precision neutron physics list utilizing cross sections from G4NDL3.14 for neutrons under 20 MeV. Four simulations, for neutrons from uranium and thorium, with the spectra from SOURCES4A and USD (shown in Figure

Three simplified direct dark matter detector geometries were established to study neutron elastic scatter signals within central detector materials and the potential for vetoing neutrons with outer detectors. The first was a spherical liquid argon detector, with a radius of 1 m, which is surrounded by shells of 10 cm thick acrylic, 5 mm thick borosilicate glass, and a water veto out to a radius of 3 m. The simulated neutrons were isotropically created in the borosilicate glass, as it is the leading source of radiogenic neutrons in many liquid argon detectors.

The second geometry studied was a cylindrical liquid xenon detector with a 1 m diameter and height. It is nested within cylinders of 3 cm thick PTFE, 2 cm thick titanium, and liquid scintillator veto with a diameter and height of 3 m. Neutrons were generated isotropically in the PTFE; it is not likely to be the leading source of neutron backgrounds for most xenon detectors but may contribute significantly to the total radiogenic neutron yield.

The final geometry studied was a cylindrical solid germanium detector with a 10 cm diameter and 120 cm height. It is surrounded by nested cylinders: first 1 cm thick copper, then 15 cm of polyethylene veto and 10 cm of lead. The neutrons are generated isotropically within the copper.

For these sample studies, an analysis threshold on the neutron-induced nuclear recoils of 20 keV was set in the argon detector and 5 keV in the xenon and germanium detectors. Scatters were rejected as WIMP-like recoils if there were multiple nuclear scatters over threshold within the target. Figure /reffig:nuclearrecoils shows the total induced nuclear recoil spectra in these simulated detector targets along with the single nuclear recoil spectra. The larger liquid noble detectors show greater reductions from all nuclear scatters to single nuclear scatters due to their size. The induced recoil spectra visibly smooth out the shape differences between the input neutron yield spectra, and the differences between simulations originating with the SOURCES4A and USD are minimized when studying the single nuclear recoils of interest.

TABLE V. The differences in nuclear recoil counts over threshold simulated for different origin and target materials with SOURCES 4A and USD initial neutron spectra and yields. The percentage difference is calculated as (SOURCES4A-USD)/[(SOURCES4A+USD)/2]. The $\chi^2$ per degree of freedom is calculated just for the single recoil spectra shape and excludes the normalization to total neutron yield.

| **Materia/Target** | **Chain** | Recoils Diff% | Singles Diff% | $\chi^2$/NDF |
|---|---|---|---|---|
| Borosilicate/Ar | $^{238}U$ | 23 | 34 | 1.24 |
| | $^{232}Th$ | 27 | 41 | 1.32 |
| PTFE/Xe | $^{238}U$ | -2 | 11 | 1.89 |
| | $^{232}Th$ | 23 | 26 | 1.06 |
| Cu/Ge | $^{238}U$ | -81 | -58 | 152 |
| | $^{232}Th$ | -16 | -14 | 5.83 |

Table V provides the percentage difference between the simulated nuclear recoil counts from SOURCES4A and USD neutron spectra. The difference in counts for the borosilicate and PTFE studies can nearly all be attributed to the difference in the total neutron yields. Indeed, these count differences are generally smoothed out and reduced proportionately from the yield differences in Table IV, and a $\chi^2$ per degree of freedom test of just the recoil spectra shapes shows reasonable agreement between both simulations.

This is not the case for the neutrons originating in copper. The total yields began with a 20% agreement, but the truncation in energy of the USD spectra causes a significant difference of up to 80% for the numbers of recoils seen above threshold. These differences are easily seen in the lower-left panel of Figure 4 for the $^{238}$U neutrons originating in Cu and recoiling in a Ge target.

Additional tests, that are not shown here, vetoed events with more than 1 keV deposited from inelastic or capture gamma ray scatters within the target, or if a neutron capture occurred within the veto material. Although no common dopants were included in the veto materials, most neutrons did capture within the vetoes. The remaining elastic nuclear scatters comparisons between SOURCES and USD initial spectra were analogous to those for the single recoils, which is why we have chosen not to add them to the plots of Figure 4.

The impact upon neutron background simulations for dark matter detectors of the difference between ($\alpha$, n) neutron spectra calculated with SOURCES4A and the USD webtool is primarily one of overall normalization. The differences would lead to different background predictions prior to running an experiment, but when spectral fits are made to recoils seen in a detector for multiple scatters, high energy or high radius events, the prediction of low energy single nuclear recoils is quite robust. However, there may be other exceptions besides copper to these spectral considerations.

## IV. CONCLUSION

The low radioactive background physics community has access to two tools for calculating $\alpha$-n neutron yield spectra for common $\alpha$-decay sources: SOURCES4A and the USDneutronyield webtool. Both codebases may meet the needs of particular users.

SOURCES4A allows the user full control of the reactions they are studying, including the ability to study the decay chains out of secular equilibrium between their early and late chains. In addition, the neutron yields from spontaneous fission are also easily calculated. However, personal correspondence with the code developers s advised for updates on extended energy ranges and corrected cross sections.

The USD webtool provides a user-friendly webform interface to quickly obtain neutron spectra with realistic resonant peaks. The lack of fission yields and options for broken equilibrium are disadvantages compared to the customizable SOURCES4A.

Between the two tools we found no systematic differences between the input cross-sections and output spectra and yields. Both may have errors in cross sections or outputs that require a human eye to catch. Low energy neutron physics codes been notoriously difficult to benchmark, and the agreement to 50% or better between these packages can probably be interpreted as bracketing the known range of neutron yields.

Once the neutron yields are used as the input to background simulations, the differences in both yield and spectral shape are smoothed away in GEANT4 Monte Carlo studies of neutron induced nuclear recoils. As common additional cuts are placed on single nuclear recoils without additional gamma ray signals from inelastic scatters or neutron capture in a veto, both SOURCES4A and USD input spectra predict similar background counts.

A complete comparison and validation of these tools would require comparison with data. However, such data sets are difficult to obtain. For a running experiment, detailed geometries of fully assayed parts would be necessary to compare against recoil spectra generated by SOURCES3A and USD. Statistical agreement with both code bases is likely with the purposefully low rates of neutron recoils within low background experiments.

SOURCES4A has a long history of use within the low background community, and will continue to be used for simulating future generations of experiments. As the newer TALYS nuclear code base that USD relies upon is exercised in other nuclear physics settings, the greater the likelihood of the USD webtool or a similar TALYS based calculation being used for radiogenic background predictions. Both will offer benefits to their users.


[1] W. Wilson, R. Perry, W. Charlton, and T. Parish, Progress in Nuclear Energy **51**, 608 (2009).

[2] D. M. Mei, C. Zhang, and A. Hime, Nucl. Instrum. Meth. **A606**, 651 (2009), arXiv:0812.4307 [nucl-ex].

[3] E.-I. statistical model code for nucelar reaction calculation, https://www-nds.iaea.org/empire218/manual.ps..

[4] A. Koning, D. Rochman, S. van der Marck, J. Kopecky, J. C. Sublet, S. Pomp, H. Sjostrand, R. Forrest, E. Bauge, and H. Henriksson, TENDL-2012: TALYS-based evaluated nuclear data library, ftp://ftp.nrg.eu/pub/www/talys/tendl2012/tendl2012.html.

[5] A. Koning and D. Rochman, Nuclear Research and Consultancy Group (NRG), http://www.talys.eu/documentation/.

[6] "Rat (is an analysis tool) users guide," `http://rat.readthedocs.org/en/latest/`, accessed: 2016-01-21.

FIG. 3. Radiogenic neutron spectra (n·MeV$^{-1}$·s$^{-1}$·cm$^{-3}$) calculated for 1ppb $^{238}$U and $^{232}$Th decay chains, left and right panels, respectively. The ($\alpha$, n) reaction contribution is shown in variuos commonly used materials from SOURCES4A in orange and USD in blue. From top to bottom materials are: copper, titanium, stainless steel, pyrex, borosilicate glass, polyethylene and teflon (PTFE).

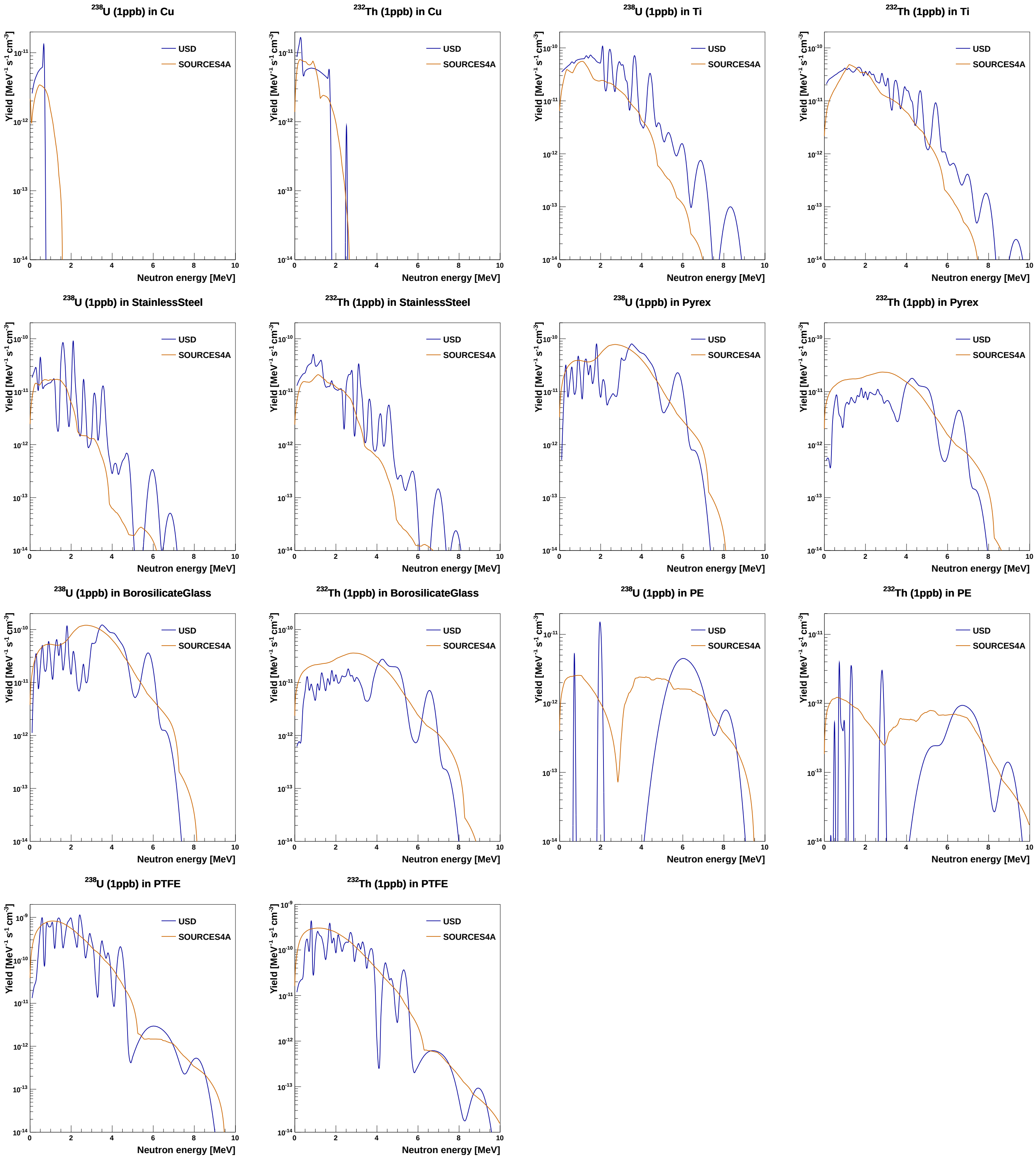

FIG. 4. Comparisons of nuclear recoils in simplified direct dark matter detector GEANT4 simulations induced from ($\alpha$, n) neutrons originating in detector materials. All orange lines correspond to SOURCES4A initial spectra, while the USD initial spectra are plotted in blue. The solid lines are histograms of all individual nuclear recoils in the target materials, while the dashed lines are irreducible single nuclear recoils within the target. On the left are simulations for $^{238}$U, and $^{232}$Th spectra are on the right. The detectors from top to bottom are an argon target with neutrons originating in borosilicate glass, a xenon target with neutrons originating in PTFE, and a germanium target with neutrons originating in copper.